Computer Assisted Mechanics and Engineering Sciences, 5: 361–372, 1998.

Vibrational power flow in beam-plate structures Part II: Beam-plate structure with isolating components

Chuijie Yi
Shandong Institute of Technology
255012 Zibo, P.R. China

Peter Dietz
Institut für Maschinenwesen, TU-Clausthal,
Robert-Koch-Str. 32, 38678 Clausthal-Zellerfeld, Germany

Xuanli Hu
AUDIAG, I/EG-31, D-85045 Ingolstadt, Germany

(Received August 22, 1997)

The expressions of vibration power flow (VPF) in beam-plate structures (BPS) have been derived in the Part I of this paper. Based on those results got in Part I, Part II presents the expressions of VPF in BPS under the following three cases as shown Figs. 1, 2 and 3 below. (1) the isolating component 1 (IC1) being added at the free end of the beam; (2) isolating component 2 (IC2) being embedded between the beam and the plate; and (3) IC1 and IC2 being in BPS simultaneously (IC1 and IC2). According to these expressions, the corresponding numerical calculations are completed. The influence of parameter of the isolating components on VPF is also considered in this part. And then numerical calculations of VPF are verified by the measurements of VPF. Some valuable conclusions have been applied to vibration control of tracked vehicles mentioned in Part I.

Key Words: Vibration Power Flow(VPF), Beam-Plate Structures and Isolation (BPS).

1. Introduction

In structural vibration problems, it is often limited for changing or adjusting the parameters of structures themselves to control structural vibration. In order to improve the quality of structural vibration control, some extra components, such bodies with isolating and dispersing performance, are usually added in structures. In traditional vibration isolation, structural vibration acceleration or velocity is used as the basis of vibration analysis and design. This is not of sufficient information to tackle the transferring paths and the distributing behavior of vibrational energy in structures. At present the problem is how to use energy method to analyze quantitatively structural vibration when the isolating components are added.

The investigation aims at the physical phenomena of VPF in BPS when the isolating components are added. If isolating components are added to the different places of BPS, such as IC1 and IC2, how does the VPF change? How do the stiffness, loss factor and mass of the isolating components influence on VPF? Undoubtedly, these approaches are very useful for controlling the motion of vibration energy between the support roller and the armored plate of tracked vehicles mentioned in Part I. The derivation of these expressions is based on those input and transfer mobility functions of the beam and the plate in Part I. The four-polar parameter method of mechanical mobility is a main tool for deriving these expressions. It should note that the only four-edge simply supported plate is involved in this part.

2. VPF IN BPS WITH IC1

In Fig. 1 the size of the beam is $l = 300$ mm (length), $w = 50$ mm (width) and $h_2 = 5$ mm (thickness). The size of the plate is $a = 1000$ mm (length), $b = 500$ mm (width) and $h_1 = 6$ mm (thickness). IC1 may be simplified as an oscillator with mass, stiffness and loss factor. If we can know the input mobility G_{I1} of the structure at the point on which the force F is exerted, the VPF which injects into the structure from IC1 is given by [1]

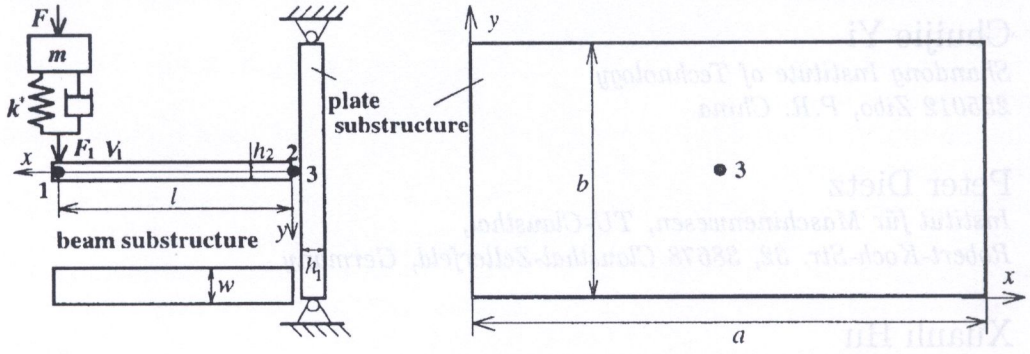

Fig. 1. BPS with IC1; beam: ($l \times w \times h_2 = 300 \times 50 \times 5$ mm); plate ($a \times b \times h_1 = 1000 \times 500 \times 6$ mm); IC1: $k^* = 1.4 \times 10^4(1 + i0.04)$ N/m, m=0.5 kg

$$P_{\text{in}} = \frac{1}{2}|F|^2 \text{Re}\{G_{I1}\}\,. \tag{1}$$

The input mobility at point 1 of the beam known in part I is given again [1]

$$G = G_{11} - [G_{12}G_{21}/(G_{22} + G_{33})]\,, \tag{2}$$

in which, G_{11}, G_{12}, G_{21} and G_{22} are the input and transfer mobilities of the beam. G_{33} is the input mobility of the plate. According to the expressions of input and transfer VPFs [1], the transfer VPF from the beam to the plate is given by

$$P_{\text{tr}} = \frac{1}{2}|F_1|^2\,|G_{21}/(G_{22} + G_{33})|^2\,\text{Re}\{G_{33}\}\,, \tag{3}$$

where F_1 is the force that IC1 exerts on the beam at point 1 and the corresponding velocity is V_1. By means of the method of four-polar parameter, the relationship between F, V and F_1, V_1 shown in Fig. 1 is expressed as [2]

$$\begin{bmatrix} F \\ V \end{bmatrix} = \begin{bmatrix} 1 & i\omega m \\ 0 & 1 \end{bmatrix} \begin{bmatrix} 1 & o \\ i\omega/k^* & 1 \end{bmatrix} \begin{bmatrix} F_1 \\ V_1 \end{bmatrix}, \tag{4a}$$

where i is unit imaginary number; m and k^* are the mass and comlex stiffness of IC1. Based on the equation above force F and velocity V are obtained by

$$F = [1 - (\omega m^2/k^*)]F_1 + i\omega m V_1, \tag{4b}$$

$$V = (i\omega/k^*)F_1 + V_1. \tag{4c}$$

Combining Eq. (4a) and Eq. (4c) and considering input mobility $G = V_1/F_1$ at point 1, force F_1 yields

$$F_1 = F\frac{1}{[1 - (\omega^2 m/k^*)] + i\omega m G}\,. \tag{5}$$

And then the total input mobility of the BPS with IC1 is given by

$$G_{I1} = \frac{V}{F} = \frac{(i\omega/k^*) + G}{[1 - (\omega^2 m/k^*)] + i\omega m G} \,. \tag{6}$$

Substituting Eq. (6) into Eq. (1), the input VPF injecting from IC1 yields

$$P_{\mathrm{tr}} = \frac{1}{2}|F|^2 \mathrm{Re}\{G\} \tag{7}$$

$$= \frac{1}{2}|F|^2 \mathrm{Re}\left\{ \frac{(i\omega/k^*) + G_{11} - [G_{12}G_{21}/(G_{22} + G_{33})]}{[1 - (\omega^2 m/k^*)] + i\omega m[G_{11} - G_{12}G_{21}/(G_{22} + G_{33})]} \right\}.$$

Substituting Eq. (5) into Eq. (3), the transfer VPF from the beam to the plate is expressed as

$$P_{\mathrm{tr}} = \frac{1}{2}|F|^2 \left| \frac{G_{21}}{G_{22} + G_{33}} \right|^2 \tag{8}$$

$$\left| \frac{1}{[1 - (\omega^2 m/k^*)] + i\omega m\{G_{11} - [G_{12}G_{21}/(G_{22} + G_{33})]\}} \right|^2 \mathrm{Re}\{G_{33}\}.$$

3. VPF IN BPS WITH IC2

As shown in Fig. 2(a), IC2 is embedded between the beam and the plate. As a result, IC2 will subject to a bending moment and produces an angle displacement. Its complex stiffness is expressed as $k_\theta^* = k_\theta(1 + i\eta_\theta)$ in which η_θ is the loss factor. In order to simplify the following expressions, the rotary inertia of IC1 and the beam are together considered as I_θ. The VPF in BPS with IC2 can be analyzed with the help of these three substructures as shown Fig. 2(b), i.e., substructure 1 (beam), substructure 2 (IC2) and substructure 3 (plate). Refer to Eqs. (1) and (3), the input and transfer VPFs may be expressed as

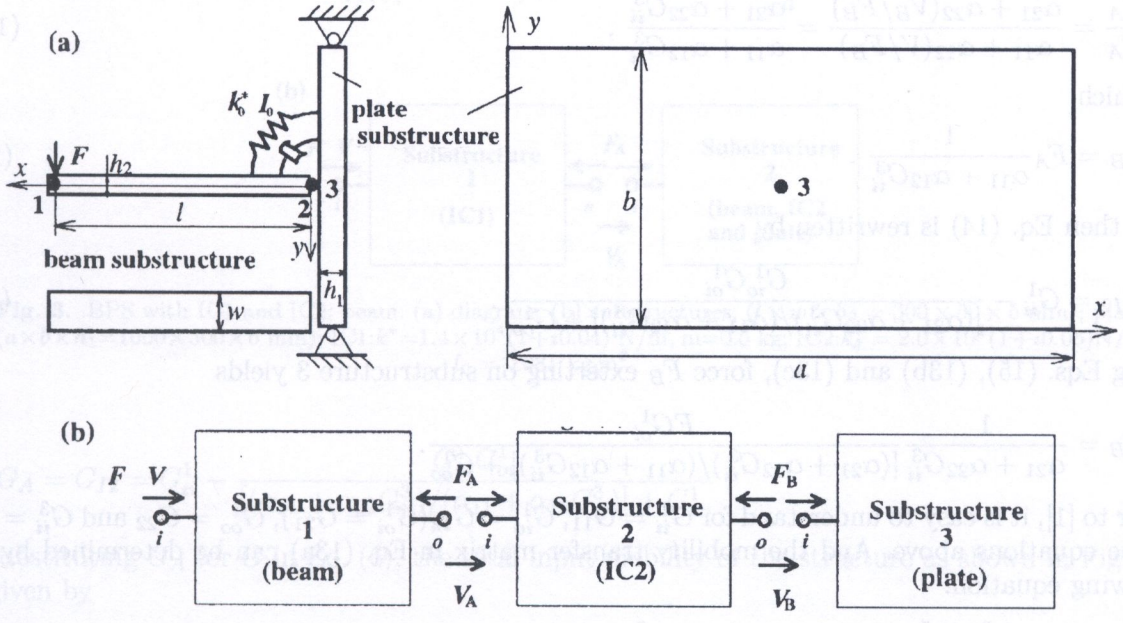

Fig. 2. BPS with IC2; (a) diagram; (b) substructures; beam: ($l \times w \times h_2 = 300 \times 50 \times 5$ mm); plate: ($a \times b \times h_1 = 1000 \times 500 \times 6$ mm); IC2: $k_\theta^* = 2.0 \times 10^4(1 + i0.06)$ N/m, $I_\theta = 0.081$ kg·m^2

$$P_{\text{in}} = \frac{1}{2}|F|^2 \text{Re}\{G_{I2}\}, \tag{9}$$

$$P_{\text{tr}} = \frac{1}{2}|F_B|^2 \text{Re}\{G^3_{ii}\}, \tag{10}$$

where G_{I2} is the total input mobility of the structure and it is defined as $G_{I2} = V/F$. In Eq. (10) G^3_{ii} is defined as $G^3_{ii} = V_B/F_B$, i.e., the input mobility at point i of substructure 3 (plate) as shown Fig. 2(b). F_B and V_B are the force and velocity between substructures 2 and 3. For substructure 1 the input and output velocities may be expressed as, respectively [1]

$$V = G^1_{ii}F - G^1_{io}F_A, \tag{11}$$

$$V_A = G^1_{oi}F - G^1_{oo}F_A, \tag{12}$$

in which the mobility terms are defined as $G^i_{jj} = V^i_j/F^i_j$ and $G^i_{jk} = V^i_j/F^i_k$. They mean respectively the input mobility of substructure i at point j and the transfer mobility of substructure i between points j and k. For substructure 2, the following matrix equations is given by

$$\begin{bmatrix} F_A \\ V_A \end{bmatrix} = \begin{bmatrix} \alpha_{11} & \alpha_{12} \\ \alpha_{21} & \alpha_{22} \end{bmatrix} \begin{bmatrix} F_B \\ V_B \end{bmatrix}, \tag{13a}$$

in which α_{11}, $\alpha_{12}(\alpha_{21})$ and α_{22} are parameters of the mobility transfer matrix. Using Eqs. (11) and (12), the total input mobility G_{12} of the structure and force F_A exterting on substructure 2 (IC2) are given by

$$G_{I2} = \frac{V}{F} = G^1_{ii} - \frac{G^1_{io}G^1_{oi}}{(V_A/F_A) + G^1_{oo}}, \tag{14}$$

$$F_A = \frac{G^1_{oi}F}{[V_A/F_A) + G^1_{oo}]}. \tag{15}$$

From Eq. (13a), V_A/F_A can be solved by

$$\frac{V_A}{F_A} = \frac{\alpha_{21} + \alpha_{22}(V_B/F_B)}{\alpha_{11} + \alpha_{12}(V/F_B)} = \frac{\alpha_{21} + \alpha_{22}G^3_{ii}}{\alpha_{11} + \alpha_{12}G^3_{ii}}, \tag{13b}$$

in which

$$F_B = F_A \frac{1}{\alpha_{11} + \alpha_{12}G^3_{ii}}. \tag{13c}$$

And then Eq. (14) is rewritten by

$$G_{I2} = G^1_{ii} - \frac{G^1_{io}G^1_{oi}}{[(\alpha_{21} + \alpha_{22}G^3_{ii})/(\alpha_{11} + \alpha_{12}G^3_{ii})] + G^1_{oo}}. \tag{16a}$$

Using Eqs. (15), (13b) and (13c), force F_B exterting on substructure 3 yields

$$F_B = \frac{1}{\alpha_{21} + \alpha_{22}G^3_{ii}} \frac{FG^1_{oi}}{[(\alpha_{21} + \alpha_{22}G^3_{ii})/(\alpha_{11} + \alpha_{12}G^3_{ii})] + G^1_{oo}}. \tag{17}$$

Refer to [1], it is easy to understand for $G^1_{ii} = G_{11}$, $G^1_{io} = G_{12}(G^1_{oi} = G_{21})$, $G^1_{oo} = G_{22}$ and $G^3_{ii} = G_{33}$ in the equations above. And the mobility transfer matrix in Eq. (13a) can be determined by the following equation.

$$\begin{bmatrix} \alpha_{11} & \alpha_{12} \\ \alpha_{21} & \alpha_{22} \end{bmatrix} = \begin{bmatrix} 1 - (\omega^2 I_\theta/k^*_\theta) & i\omega I_\theta \\ (i\omega/k^*_\theta) & 1 \end{bmatrix}. \tag{18}$$

Substituting Eq. (16a) into Eq. (9) and Eq. (17) into Eq. (10), considering Eq. (18), the input and transfer VPFs in BPS with IC2 are given by

$$P_{\text{in}} = \frac{1}{2}|F|^2 \text{Re}\left\{ G_{11} - \frac{G_{12}G_{21}}{G_{22} + \{[i\omega/k_\theta^*) + G_{33}] \,/\, [1 - (\omega^2 I_\theta / k_\theta^*) + i\omega I_\theta G_{33}]\}} \right\} \tag{19}$$

$$P_{\text{tr}} = \frac{1}{2}|F|^2 \left| \frac{1}{1 - (\omega^2 I_\theta / k_\theta^*) + i\omega I_\theta G_{33}} \right|^2 \tag{20}$$

$$\left| \frac{G_{21}}{G_{22} + \{[(i\omega/k^*) + G_{33}]/[1 - (\omega^2 I_\theta / k_\theta^*) + i\omega I_\theta G_{33}]\}} \right|^2 \text{Re}\{G_{33}\} \,.$$

4. VPF BPS WITH IC1 AND IC2

Figure 3(a) shows a diagram of the BPS with IC1 and IC2. IC1 is added at the free end of the beam and IC2 is embedded between the beam and the plate. In Fig. 3(b) substructure 1 represents IC1 and Substructure 2 includes the beam, IC2 and the plate, i.e., the structure as shown in Fig. 2(a). The input mobility of substructure 2 is equivalent to the input mobility expressed by Eq. (16a), i.e.,

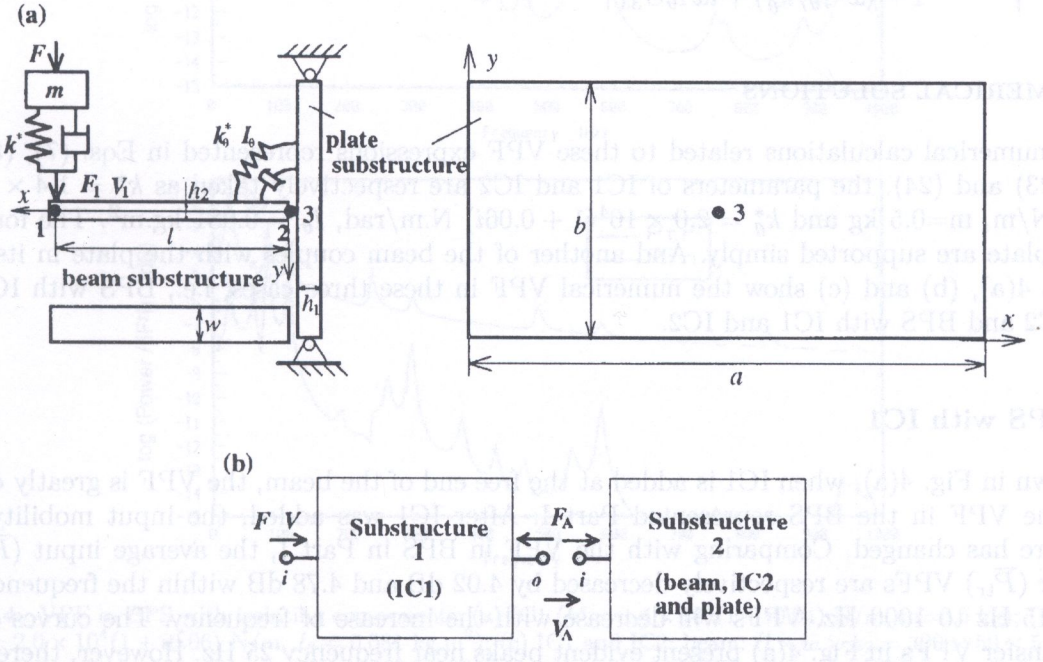

Fig. 3. BPS with IC1 and IC2; beam: (a) diagram; (b) substructures; ($l \times w \times h_2 = 300 \times 50 \times 5$ mm); plate: ($a \times b \times h_1 = 1000 \times 500 \times 6$ mm); IC1:$k^* = 1.4 \times 10^4(1 + i0.04)$ N/m, m=0.5 kg; IC2:$k_\theta^* = 2.0 \times 10^4(1 + i0.06)$N/m, $I_\theta = 0.081$ kg·m^2

$$G_A = G_{I2} = G_{ii}^1 - \frac{G_{io}^1 G_{oi}^1}{[(\alpha_{21} + \alpha_{22} G_{ii}^3)/(\alpha_{11} + \alpha_{12} G_{ii}^3)] + G_{oo}^1} \,. \tag{16b}$$

If substituting G_A for G in Eq. (6), the total input mobility of the structure as shown in Fig. 3(a) is given by

$$G_{II} = \frac{V}{F} = \frac{(i\omega/k^*) + G_A}{[1 - (\omega^2 m/k^*)] + i\omega m G_A} \,. \tag{21}$$

And then substituting G_A for G in Eq. (5), we will get force F_A which exerts on substructure 2 in Fig. 3(b). Actually it is equal to force F_1 which exerts on the free end of the beam.

$$F_A = F_1 = F\frac{1}{[1-(\omega^2 m/k^*)] + i\omega m G_A} \,. \tag{22}$$

Substituting Eq. (21) into Eq. (1), the input VPF is given by

$$P_{\text{in}} = \frac{1}{2}|F|^2 \text{Re}\{G_{II}\} = \frac{1}{2}|F|^2 \text{Re}\left\{\frac{(i\omega/k^*) + G_A}{[1-(\omega^2 m/k^*)] + i\omega m G_A}\right\} \,, \tag{23}$$

in which G_A is determined by Eq. (16b). Substituting Eq. (22) into Eq. (3), the transfer VPF from IC2 to the plate is also given by

$$P_{\text{tr}} = \frac{1}{2}|F|^2 \left|\frac{1}{\left(1-\dfrac{\omega^2 m}{k^*}\right) + i\omega m G_A}\right|^2 \left|\frac{1}{\left(1-\dfrac{\omega^2 I_\theta}{k_\theta^*}\right) + i\omega I_\theta G_{33}}\right|^2 \left|\frac{G_{21}}{G_{22} + \dfrac{(i\omega/k_\theta^*) + G_{33}}{1-(\omega^2 I_\theta/k_\theta^*) + i\omega I_\theta G_{33}}}\right|^2 \text{Re}\{G_{33}\} \,. \tag{24}$$

5. Numerical solutions

In the numerical calculations related to these VPF expressions represented in Eqs. (7), (8), (19), (20), (23) and (24), the parameters of IC1 and IC2 are respectively taken as $k^* = 1.4 \times 10^4(1 + 0.04i)$ N/m, m=0.5 kg and $k_\theta^* = 2.0 \times 10^4(1 + 0.06i)$ N.m/rad, $I_\theta = 0.081$ kg.m^2. The four edges of the plate are supported simply. And another of the beam couples with the plate in its center. Figures 4(a), (b) and (c) show the numerical VPF in these three cases, i.e., BPS with IC1, BPS with IC2 and BPS with IC1 and IC2.

5.1. BPS with IC1

As shown in Fig. 4(a), when IC1 is added at the free end of the beam, the VPF is greatly different from the VPF in the BPS represented Part I. After IC1 was added, the input mobility of the structure has changed. Comparing with the VPF in BPS in Part I, the average input ($\overline{P}_{\text{in}}$) and transfer ($\overline{P}_{\text{tr}}$) VPFs are respectively decreased by 4.02 dB and 4.78 dB within the frequency range from 115 Hz to 1000 Hz. VPFs will decrease with the increase of frequency. The curves of input and transfer VPFs in Fig. 4(a) present evident peaks near frequency 25 Hz. However, there are not the peaks in Fig. 4(b) at the same frequency. This is reason that the natural frequency of IC1 is just equal to 26.6 Hz. This results in the input VPF to be amplified below 40 Hz.

5.2. BPS with IC2

Because IC2 is embedded between beam and plate, the relationship among the mobilities related to beam and plate have changed. This makes the transferring ability of the VPF from beam to plate to decrease greatly. It is seen that $\overline{P}_{\text{tr}}$ in Fig. 4(b) is much less than that in Fig. 4(a). In frequency range of 115 Hz–1000 Hz, for instance, $\overline{P}_{\text{tr}}$ in Fig. 4(b) is decreased by 5.18 dB, but $\overline{P}_{\text{tr}}$ Fig. 4(a) is only decreased by 3.04 dB. The natural frequency of IC2 is 79 Hz. The transfer VPF is also amplified below frequency 112 Hz.

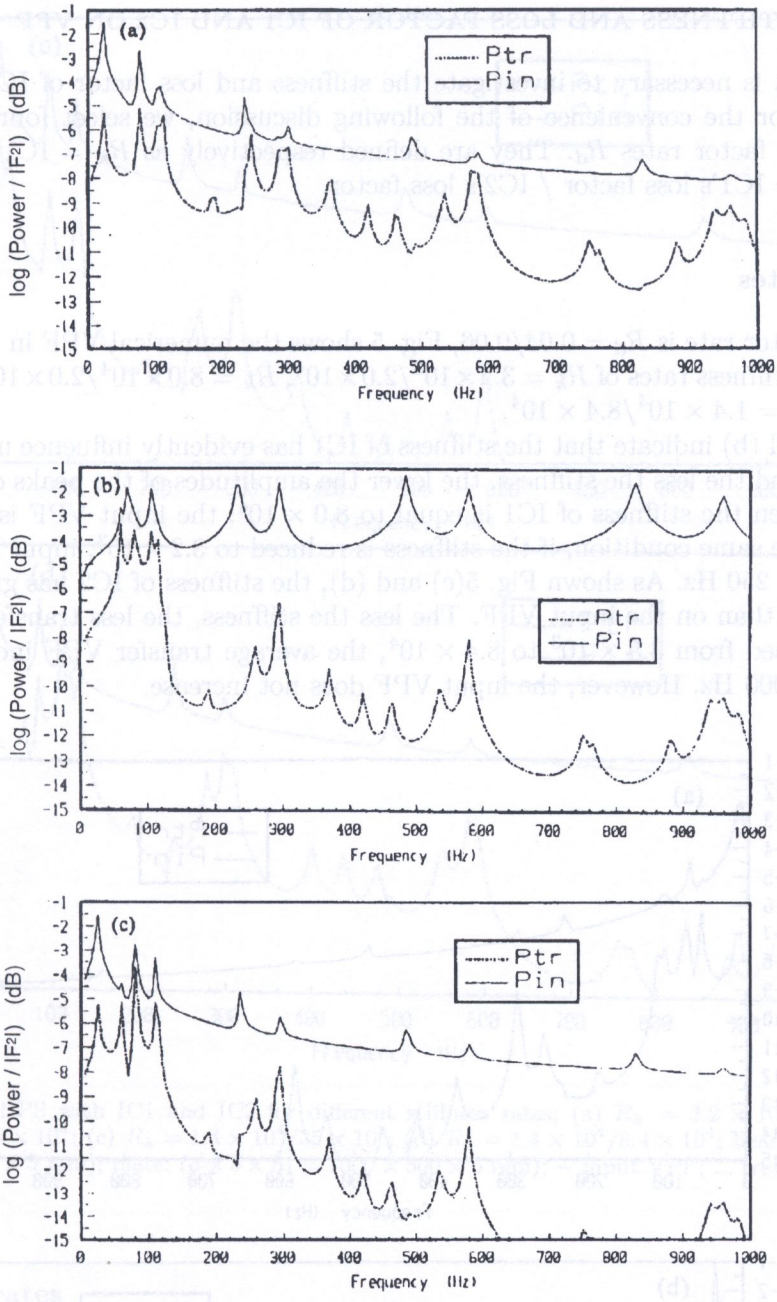

Fig. 4. VPF in BPS with isolating components; (a) IC1 ($k^* = 1.4 \times 10^4(1 + i0.04)$ N/m, m=0.5 kg); (b) IC2 ($k_\theta^* = 2.0 \times 10^4(1 + i0.06)$ N/m, $I_\theta = 0.081$ kg.m^2); (c) IC1 and IC2; beam: ($l \times w \times h_2 = 300 \times 50 \times 5$ mm); plate: ($a \times b \times h_1 = 1000 \times 500 \times 6$ mm); – input VPF; ... transfer VPF

5.3. BPS with IC1 and IC2

As shown in Fig. 4(c), the input and the transfer VPFs all are decreased greatly over 112 Hz in the frequency range of interest. The higher the frequency, the greater the decrease of VPFs. Comparing with the VPFs in the BPS in part I, $\overline{P}_{\text{in}}$ and $\overline{P}_{\text{tr}}$ are decreased respectively by 4.07 dB 6.31 dB. In this case $\overline{P}_{\text{tr}}$ is 1.53 dB less than that the in the case of IC1. However, comparing with the VPFs in the case of IC2, $\overline{P}_{\text{tr}}$ are only decreased by 3.02 dB and 1.13 dB. The transfer VPF decreases not as great as the input VPF. It is seen that IC2 is nearly of the same ability with IC1 and IC2 to suppress the transfer VPF.

6. Effect of stiffness and loss factor of IC1 and IC2 on VPF

Technologically, it is necessary to investigate the stiffness and loss factor of IC1 and IC2 how to influence VPF. For the convenience of the following discussion, we select four different stiffness rates R_k and loss factor rates R_d. They are defined respectively as R_k = IC1's stiffness / IC2's stiffness and R_d = IC1's loss factor / IC2's loss factor.

6.1. Stiffness rates

When the loss factor rate is $R_d = 0.04/0.06$, Fig. 5 shows the numerical VPF in BPS with IC1 and IC2 for different stiffness rates of $R_k = 3.2\times10^3/2.0\times10^4$, $R_k = 8.0\times10^4/2.0\times10^4$, $R_k = 1.4\times10^4/3.5\times10^3$ and $R_k = 1.4\times10^4/8.4\times10^4$.

Figure 5(a) and (b) indicate that the stiffness of IC1 has evidently influence upon the input and transfer VPFs. And the less the stiffness, the lower the amplitudes of the peaks on the VPF curves in the figure. When the stiffness of IC1 is equal to 8.0×10^4, the input VPF is less than 10^{-7} at 700 Hz. Under the same condition, if the stiffness is reduced to 3.2×10^3, input VPF has been less than 10^{-7} only at 250 Hz. As shown Fig. 5(c) and (d), the stiffness of IC2 has greater influence on the transfer VPF than on the input VPF. The less the stiffness, the less transfer VPF. When the stiffness is increased from 3.5×10^3 to 8.4×10^4, the average transfer VPF increases by 2.20 dB from 250 Hz to 1000 Hz. However, the input VPF does not increase.

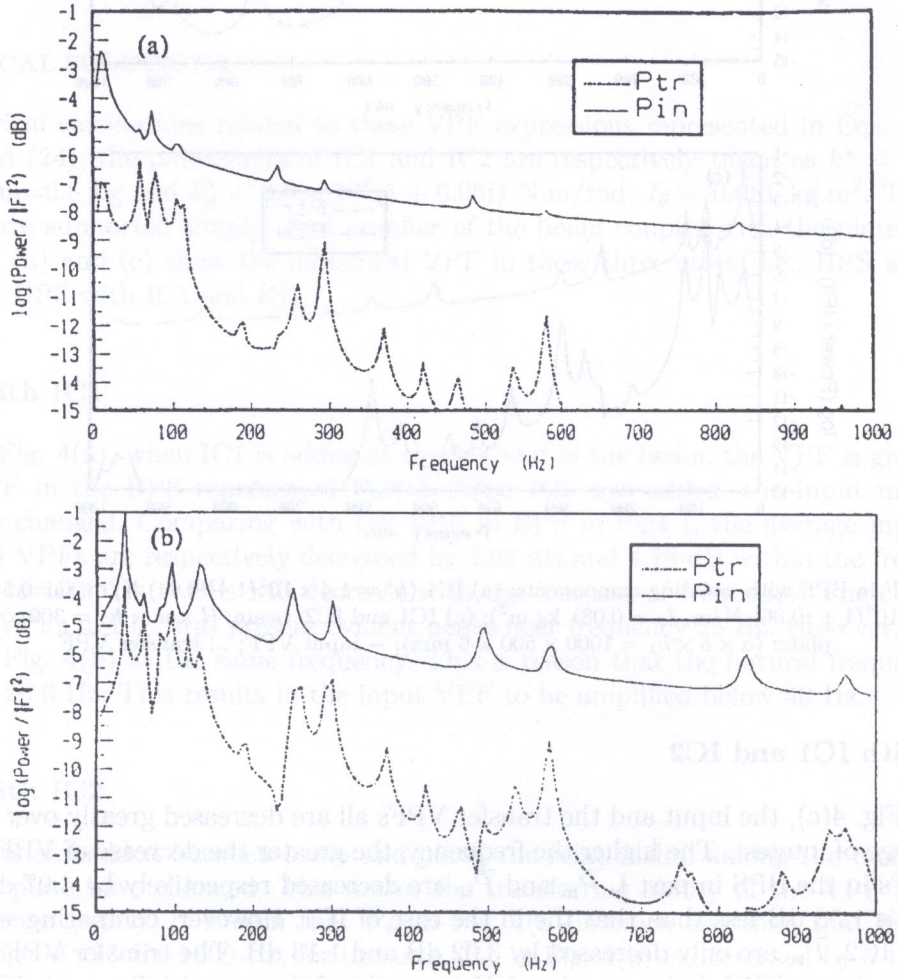

[Fig. 5 (a), (b)]

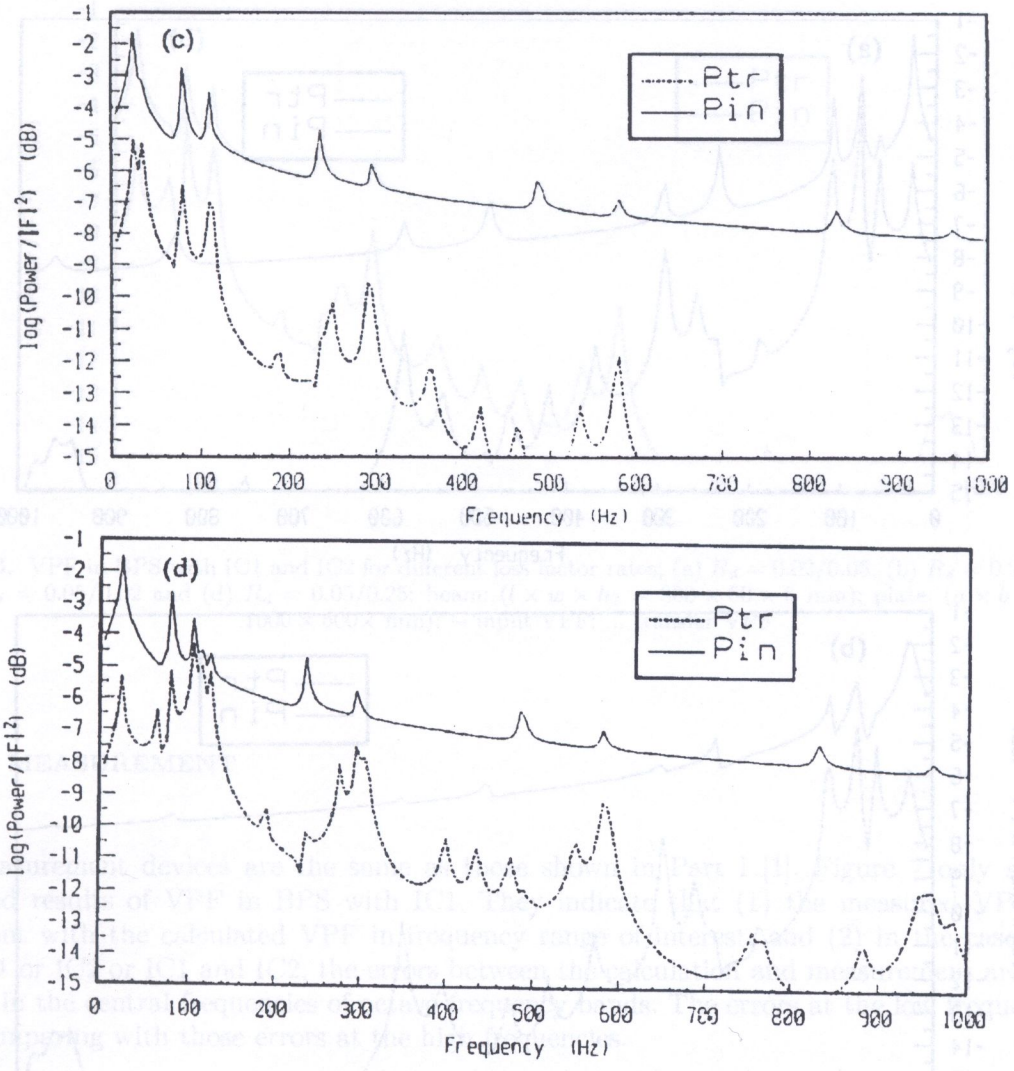

Fig. 5. VPF in BPS with IC1 and IC2 for different stiffness rates; (a) $R_k = 3.2 \times 10^3/2.0 \times 10^4$; (b) $R_k = 8.0 \times 10^4/2.0 \times 10^4$; (c) $R_k = 1.4 \times 10^4/35 \times 10^3$; (d) $R_k = 1.4 \times 10^4/8.4 \times 10^4$; beam: $(l \times w \times h_2 = = 300 \times 50 \times 5$ mm); plate: $(a \times b \times h_1 = 1000 \times 500 \times 6$ mm); – input VPF; ... transfer VPF

6.2. Loss factor rates

When the stiffness rate is $R_k = 1.4 \times 10^4/2.0 \times 10^4$, the following loss factor rates are selected, i.e., $R_d = 0.02/0.05$, $R_d = 0.25/0.05$, $R_d = 0.05/0.02$ and $R_d = 0.05/0.25$. The numerical VPF in BPS with IC1 and IC2 are shown in Fig. 6.

As shown in Fig. 6(a) and (b), to increase the loss factor of IC1 will make the amplitudes of these peaks on the curves of the input VPF to decrease. Comparing Fig. 6(a) with (b), when the loss factor of IC1 is increased to 0.25, while the input VPF is reduced to 10^{-7}, the frequency has highly been at 700 Hz. Therefore, if trying to reduce the input VPF at high frequency, we should decrease the loss factor of IC1. The loss factor of IC1 has less influence on the transfer VPF at high frequency. Figure 6(c) and (d) show the loss factor of IC2 has slightly influence on the input and transfer VPFs. It only influences the transfer VPF near natural frequency of IC2. The input VPF is nearly unchangeable from 250 Hz to 1000 Hz. And the transfer VPF is only increased by 0.11 dB.

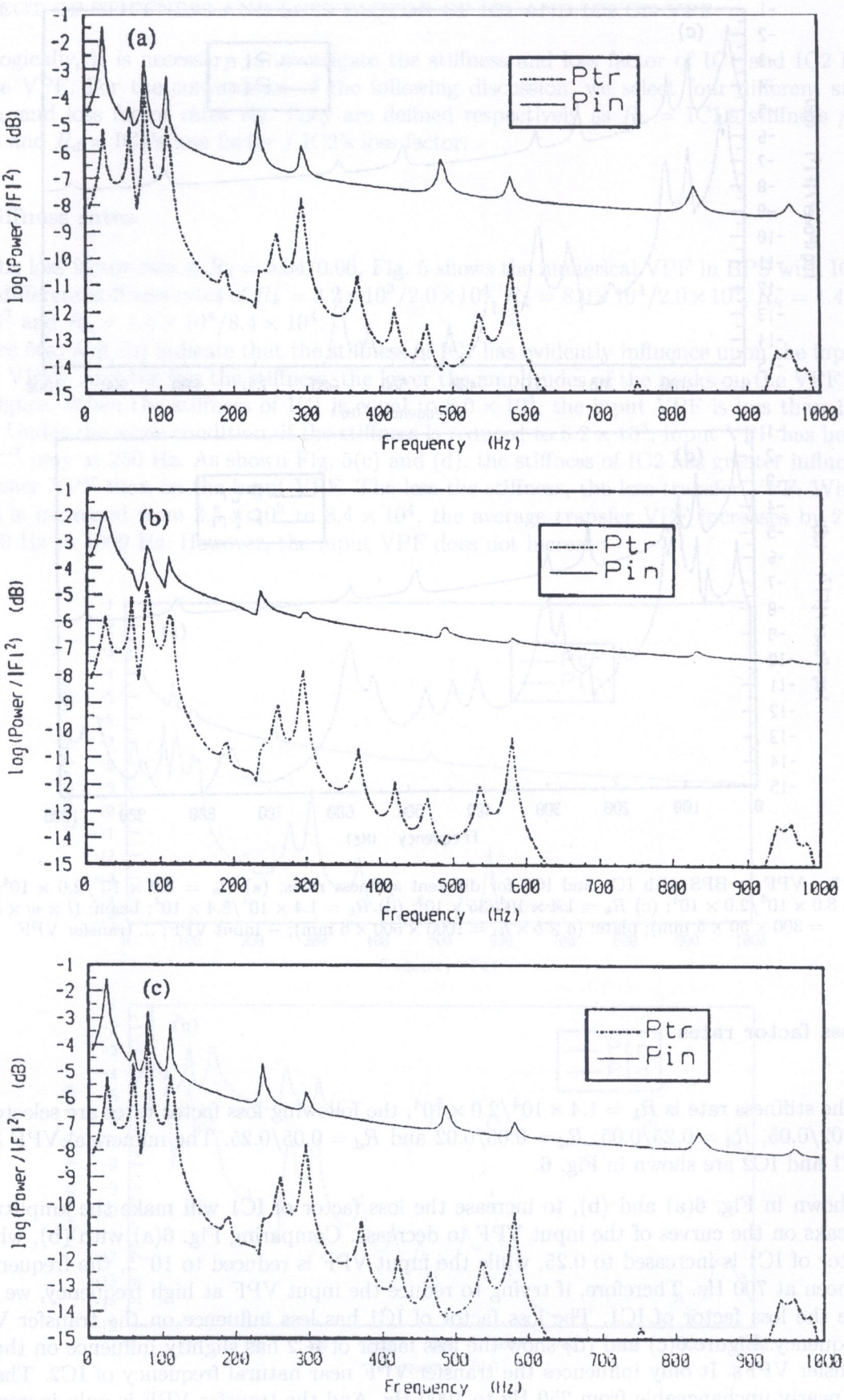
(a)
Ptr
Pin
log(Power/|F|²) (dB)
Frequency (Hz)
(b)
Ptr
Pin
log(Power/|F|²) (dB)
Frequency (Hz)
(c)
Ptr
Pin
log(Power/|F|²) (dB)
Frequency (Hz)

[Fig. 6 (a), (b), (c)]

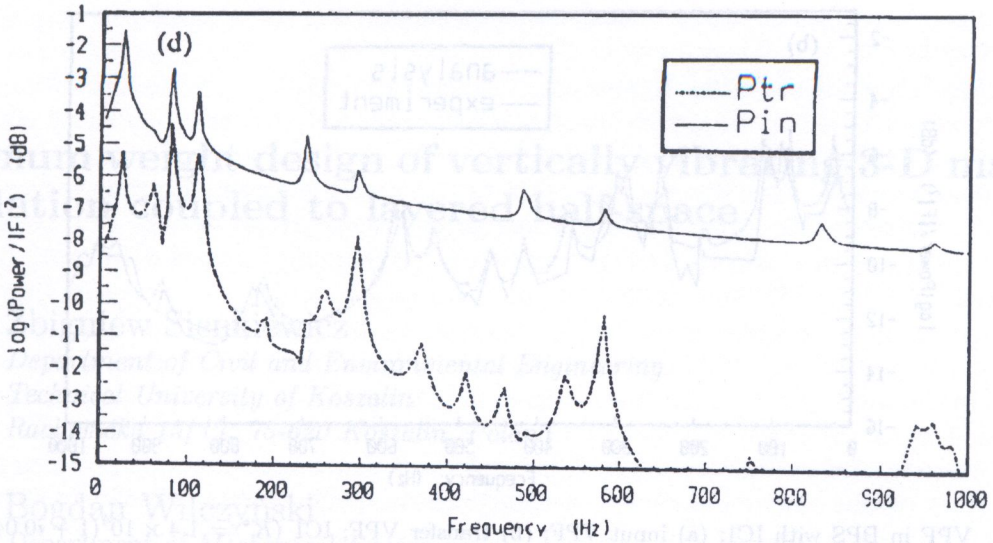

Fig. 6. VPF in BPS with IC1 and IC2 for different loss factor rates; (a) $R_d = 0.02/0.05$, (b) $R_d = 0.25/0.05$, (c) $R_d = 0.05/0.02$ and (d) $R_d = 0.05/0.25$; beam: $(l \times w \times h_2 = 300 \times 50 \times 5$ mm); plate: $(a \times b \times h_1 = 1000 \times 500\times$ mm); – input VPF; ... transfer VPF

7. VPF MEASUREMENT

The measurement devices are the same as those shown in Part I [1]. Figure 7 only shows the measured results of VPF in BPS with IC1. They indicate that (1) the measured VPF has an agreement with the calculated VPF in frequency range of interest; and (2) in the cases of BPS with IC1 or IC2 or IC1 and IC2, the errors between the calculation and measurement are listed in Table 1 in the central frequencies of octave frequency bands. The errors at the low frequencies are great comparing with those errors at the high frequencies.

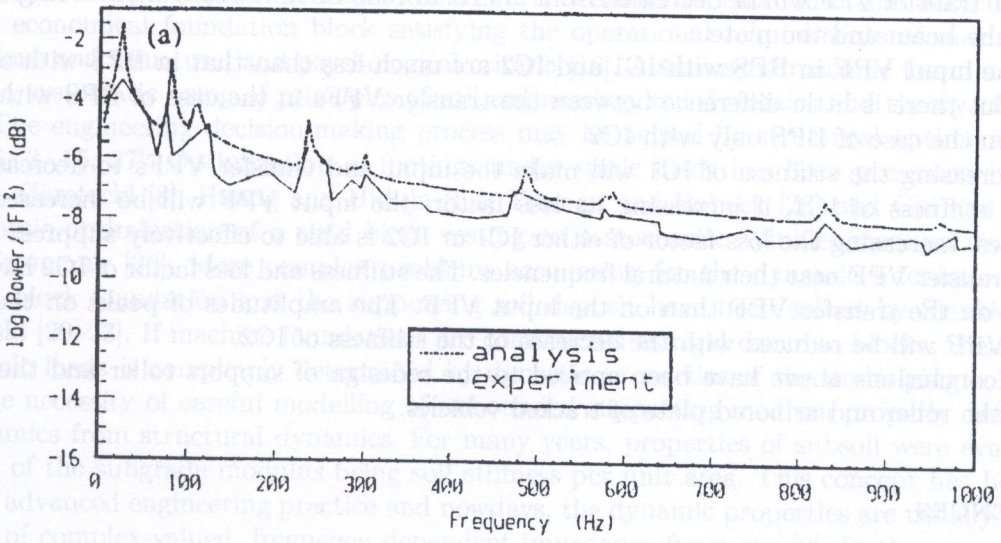

[Fig. 7 (a)]

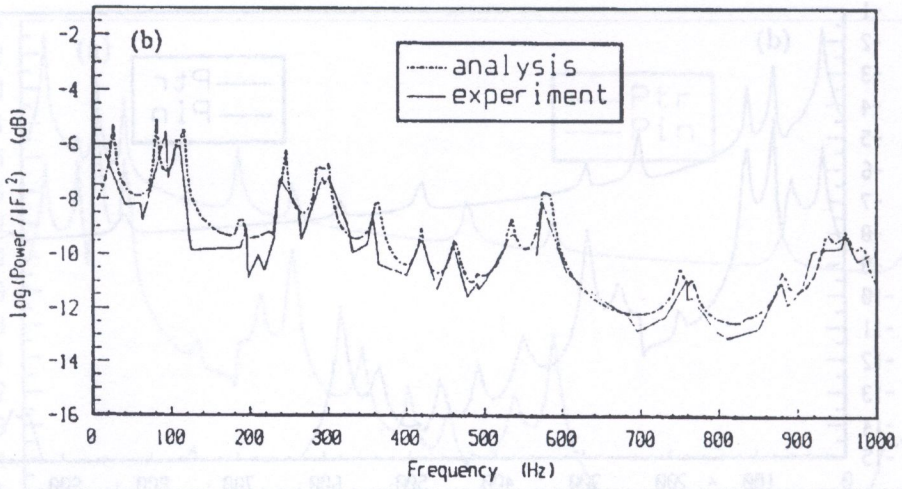

Fig. 7. VPF in BPS with IC1; (a) input VPF; (b) transfer VPF; IC1 ($K^* = 1.4 \times 10^4(1 + i0.04)$ N/m, m=0.5 kg); beam: ($l \times w \times h_2 = 300 \times 50 \times 5$ mm); plate: ($a \times b \times h_1 = 1000 \times 500 \times 6$ mm); – measurement · · · calculation

Table 1. Errors between the measurement and calculation of VPF

Central Frequencies (Hz)	31.5		63		125		250		500		1000	
	P_{in}	P_{tr}	P_{in}	P_{tr}	P_{in}	P_{tr}	P_{in}	P_{tr}	P_{in}	P_{tr}	P_{in}	P_{tr}
BPS with IC1 (%)	54	10	30	42	7	2	6	8	7	5	7	3
BPS with IC2 (%)	18	7	20	31	19	6	23	3	6	3	11	2
BPS with IC1 and IC2 (%)	80	22	45	20	2	10	6	5	8	5	7	6

8. Conclusions

(1) When IC1 is at the free end of the beam, the input and transfer VPFs can be reduced over 40 Hz.

(2) The transfer VPF will be decreased from 115 Hz to 1000 Hz in the case of IC2 being embedded between the beam and the plate.

(3) The input VPF in BPS with IC1 and IC2 are much less than that in BPS with either IC1 or IC2. But there is little difference between the transfer VPFs in the case of BPS with IC1 and IC2 and in the case of BPS only with IC2.

(4) Increasing the stiffness of IC1 will make the input and transfer VPFs to decrease. Under a certain stiffness of IC1, if increasing its loss factor, the input VPF will be increased at high frequencies. Increasing the loss factor of either IC1 or IC2 is able to effectively suppress the input and the transfer VPF near their natural frequencies. The stiffness and loss factor of IC2 have greater influence on the transfer VPF than on the input VPF. The amplitudes of peaks on the curve of transfer VPF will be reduced with the decrease of the stiffness of IC2.

Some conclusions above have been applied to the redesign of support roller and the isolation between the roller and armored plate of tracked vehicles.

References

[1] C. Yi, P. Dietz and X. Hu. Vibrational power flow in beam-plate structures, Part I: basic theory, *Computer Assisted Mechanics and Engineering Sciences*, **5**: 345–359, 1998.

[2] H. Zuo. *Analytical Method and Practical Application of Mechanical Impedance*, China Machine Press, 1st edition, 1987.